Design of artificial metalloenzymes for the reduction of nicotinamide cofactors

*Mattias Basle[a,§], Henry A. W. Padley[a,§], Floriane L. Martins[a], Gerlof Sebastiaan Winkler[b], Christof M. Jäger[a], Anca Pordea[a]**

[a]Sustainable Process Technologies, Faculty of Engineering, University of Nottingham, Nottingham, United Kingdom

[b]School of Pharmacy, University of Nottingham, Nottingham, United Kingdom

§ These authors contributed equally to the work.

Keywords: artificial metalloenzymes, alcohol dehydrogenase, cofactor regeneration

Abstract

Artificial metalloenzymes result from the insertion of a catalytically active metal complex into a biological scaffold, generally a protein devoid of other catalytic functionalities. As such, their design requires efforts to engineer substrate binding, in addition to accommodating the artificial catalyst. Here we constructed and characterised artificial metalloenzymes using alcohol dehydrogenase as starting point, an enzyme which has both a cofactor and a substrate binding pocket. A docking approach was used to determine suitable positions for catalyst anchoring to single cysteine mutants, leading to an artificial metalloenzyme capable to reduce both natural cofactors and the hydrophobic 1-benzylnicotinamide mimic. Kinetic studies revealed that the new construct displayed a Michaelis-Menten behaviour with the native nicotinamide cofactors, which were suggested by docking to bind at a surface exposed site, different compared to their native binding position. On the other hand, the kinetic and docking data suggested that a typical enzyme behaviour was not observed with the hydrophobic 1-benzylnicotinamide mimic, with which binding events were plausible both inside and outside the protein. This work demonstrates an extended substrate scope of the artificial metalloenzymes and provides information about the binding sites of the nicotinamide substrates, which can be exploited to further engineer artificial metalloenzymes for cofactor regeneration.

1 Introduction

Artificial metalloenzymes (ArMs) offer exciting opportunities to introduce non-biological reactivity into biomolecules, by taking advantage of both synthetic and natural functionalities for catalyst design.[1] The most versatile ArMs to date are based on non-enzymatic proteins, such as streptavidin[2] or the multidrug resistance regulator LmrR.[3] The use of natural enzymes as starting points for ArM design has also been reported, for example by replacing the metal in the native heme cofactor of P450s[4] or in the metal-binding site of carbonic anhydrase.[5] The advantage of such systems is that they provide a hydrophobic substrate-binding site, which is already evolved to position, orient and activate the substrate *via* specific (polar) interactions, thus conferring enzyme-like features to the ArM design. On the other hand, the high specificity and the tight control exerted by natural enzymes results in limited space availability for a non-native catalytic functionality in proximity of the substrate-binding site. The use of cofactor-dependent enzymes, which possess a binding site for an organic cofactor in addition to the substrate pocket, provides a solution to accommodate small non-biological molecule catalysts within existing enzymes.[6]

In our efforts to design ArMs from cofactor-dependent enzymes, we previously selected a member of the medium-chain zinc-dependent alcohol dehydrogenase family, namely ADH from *Thermoanaerobacter brockii* (TbADH). This enzyme has a nicotinamide cofactor ($NADP^+$) binding site, in combination with a catalytic site consisting of a hydrophobic pocket for an alcohol substrate and a metal binding pocket for a zinc ion. In our initial design, we reasoned that the hydrophobic catalytic site offers the necessary space to accommodate a non-biological organometallic complex, without disturbing the nicotinamide cofactor binding. Using this approach, our group recently reported a TbADH-based ArM for the reduction of $NADP^+$ with rhodium bipyridine or phenanthroline complexes.[7] This artificial formate dehydrogenase was

used in a coupled system with wild-type TbADH, for the *in situ* recycling of NADPH during the reduction of 4-phenyl-2-butanone into its corresponding (*S*)-alcohol. The ArM was developed using a covalent binding approach: the single cysteine mutant TbADH 5M was developed, in which the cysteine at position 37 from the zinc binding site was used as the anchoring point for the metal complexes, whilst the other three native cysteines at positions 203, 283 and 295 were mutated into alanine or serine residues. Two other alanine mutations were introduced at positions 59 and 150 in order to remove the zinc binding site and to free the space for the rhodium catalysts. The advantage of the ArMs over the free Rh catalyst was demonstrated by the ability of the protein scaffold to shield the metal complex from interacting with the native TbADH during the recycling experiments, thus resulting in increased stability of both the complex and the TbADH during ketone reduction experiments.

In our published work, the covalent bioconjugation of Rh complexes to C37 resulted in mixtures of labelled and non-labelled protein, suggesting that the thiol alkylation was not complete. Complete alkylation of the C37 had previously been reported with iodoacetic acid,[8] which indicated that the lack of space around position 37 is likely to be responsible for the incomplete labeling with the bulky organometallic moieties. Moreover, the low activity observed with the resulting ArMs also suggested that steric hindrance prevented nicotinamide binding in the native position. The importance of the anchoring position within the protein during the creation of ArMs by covalent modification was previously demonstrated. For example, when anchoring Cu(II)-phenanthroline catalysts to single cysteines in the αRep scaffold, the enantioselectivity of the Diels-Alder catalysis depended on the cysteine position.[9] Similarly, incorporation of (2,2-bipyridin-5yl)alanine, a metal-binding unnatural amino acid at different positions of the multidrug

resistance regulators QacR, RamR or CgmR led to differences in yields and enantioselectivities for Friedel-Crafts alkylation.[10]

Furthermore, the question arose whether the ADH-based artificial metalloenzymes would be able to reduce other nicotinamide derivatives. Synthetic nicotinamide cofactor biomimetics are less costly and more stable versions of their natural counterparts and are accepted by a range of oxidoreductases.[11] Chemical catalysts developed for the regeneration of the natural cofactors NADH and NADPH in the presence of formate[12] have already been shown to reduce other nicotinamide-containing compounds, albeit with lower efficiency (about 2.5 times lower).[13] Ward and co-workers have also developed ArMs based on biotinylated Ir(III)-*N*-sulfonyl-ethylenediamine complexes incorporated into streptavidin, for the regeneration of NAD(P)H and their mimics when combined with ene reductases, oxidases, oxygenases and glucose dehydrogenase.[14] Our previously published results indicated that the specificity for $NADP^+$ observed with the wild-type TbADH was not always translated to the ArMs, with similar activities being measured for the reduction of $NADP^+$ and NAD^+. Again, this suggested that the nicotinamide substrate was not bound at its native binding site.

With this in mind, the aim of the current work is to gain a better understanding of nicotinamide reduction catalysed by the TbADH-based artificial metalloenzymes. In particular, an understanding of the substrate scope and its binding to the active site of the ArMs is needed in order to engineer these entities towards better functionality. We hypothesized that the $NADP^+$ cofactor site may offer more space than the hydrophobic substrate pocket, for the binding of the organometallic moiety. With the non-native catalyst positioned in the cofactor site, there would in turn be more space for nicotinamide mimics to bind to the hydrophobic substrate pocket. Therefore, we first evaluate the effect of the cysteine position within the $NADP^+$ cofactor binding

site of TbADH on its ability to accommodate a non-natural functionality. The mutant yielding the best bioconjugation results is then tested in the reduction of $NADP^+$, NAD^+ and 1-benzylnicotinamide, a hydrophobic nicotinamide cofactor mimic. Docking studies are performed to shed light on the mode of binding of the nicotinamide substrates to the artificial metalloenzymes.

2 Materials and Methods

2.1 Computational docking

The Glide docking procedure within the Maestro software (Glide 6.7; Maestro 11.6) was used to perform non-covalent and covalent docking, with the default parameters as defined in the Schrödinger program.[15] From the crystal structure of wild-type TbADH (PDB 1YKF[16]), the following mutations were created: H59A, D150A, C203S, C283A and C295A. The catalytic zinc ion was removed from the file, to yield the structure TbADH 5M. The cysteine in position 37 was mutated to alanine to provide the scaffold TbADH 6M. Single cysteine mutations were subsequently introduced at the required positions to create several TbADH 7M scaffolds (174, 175, 178, 198, 203, 242, 243 and 266). Each mutant was prepared by using the Maestro Protein Preparation Wizard in the Schrödinger suite. Missing hydrogen atoms and side chains were added to the structure by Prime-refinement throughout the pre-processing.[15] During the refinement, water molecules with less than three hydrogen bonds to other atoms were removed, which resulted in no water in the binding site. The protonation/tautomer states and the "flip" assignment of aspartate, glutamate, arginine, lysine and histidine were adjusted at pH = 7.0 using PROPKA, in order to select the position of hydroxyl and thiol hydrogen.[17] Finally, the structures were geometrically optimized using the OPLS3 force field[18] with a RMSD = 0.3 Å displacement of non-hydrogen atoms as convergence parameter. Ligands **L1, L2, L3** benzylnicotinamide (**BNA^+**), **NAD^+** and **$NADP^+$** were prepared using the Ligprep tool from the Schrödinger suite, with the

OPLS3 force field. Generation of all possible protonation and ionisation states combinations was performed by using Epik in aqueous solution at pH of 7.0 +/- 2.0. The metal complex Cp*Rh(**L3**)H was built from the **L3** structure by using the Maestro interface to build a pyramidal metal centre, substituted by a pentamethyl cyclopentadienyl moiety (Cp*) and hydrogen. The structure was then minimized through "minimized selected atoms" task on Maestro workspace. Ligand **L1** and the complex Cp*Rh(**L3**)H were covalently docked into TbADH 7M using Glide SP procedure in Maestro, with the grid centre for the docking defined by the corresponding cysteine residue at the centre of the grid and using the template of a nucleophilic substitution between the bromide functionality and the corresponding thiol. For this step the receptor was kept rigid. The structure with the best Glide refined by Prime score was used as the receptor for the covalently bound ligand poses and for the following non-covalent docking.

For non-covalent docking of **BNA**$^+$, **NAD**$^+$ and **NADP**$^+$ the grid for the docking site was defined from the optimized protein structure at the centroid of the active site (10 Å radius around the co-crystallized NADPH ligand). The standard settings of a van der Waals scaling factor of 1.0 for nonpolar atoms was conserved and no constraints were added. Nonpolar atoms were defined with absolute value of partial atomic charges ≤ 0.25 [e]. The structure was first docked with Glide SP score then with the more accurate Glide XP score, ranking the affinity (or binding free energy) of ligands for the enzyme. For each non-covalent docking, the structure with the best Glide XP score was used for analysis.

2.2 Bioconjugation of ligands and complexes to TbADH variants

*Bioconjugation with ligands **L1, L2, L3.*** The optimized procedure was as follows. Ligand **L1, L2** or **L3** (100 μM) was mixed with the TbADH variant (5M, 6M, 7M-C174, 7M-C198, 7M-C203, 7M-C242 or 7M-C243; 25 μM, 1 mg mL^{-1}) in Tris HCl 100 mM buffer pH 8.0 for 4 h at 37 °C.

Once the bioconjugation was finished, the buffer of the resulting mixture was exchanged to ultrapure (Milli-Q®) water by passing through a PD-10 desalting column (GE Healthcare). Fractions resulting from the purification were analysed by UV-Vis, the fractions of interest were pooled and concentrated using Vivaspin 6 (10 000 MWCO; Sartorius Stedim Biotech). The final protein concentration was assayed by the Bradford method and the ratio of free thiol available within each protein sample was evaluated by Ellman's assay. The bioconjugation product was analysed by ESI-TOF using a Brucker Impact II spectrometer.

*Bioconjugation with metal complexes [Cp*Rh(**L2**)Cl]$^+$ and [Cp*Rh(**L3**)Cl]$^+$.* Complex [Cp*Rh(**L2**)Cl]$^+$ or [Cp*Rh(**L3**)Cl]$^+$ (400 μM, 4 eq.) was mixed with the TbADH variant (5M, 6M, 7M-C174 or 7M-C243; 100 μM, 4 mg mL^{-1}) in Tris HCl 100 mM buffer pH 7.0 for 1 h at room temperature. After completion, each bioconjugation product was purified and analysed as described above. ICP-MS analysis was performed to evaluate the metal content of each sample, using an iCAP-Q instrument (Thermo Fisher Scientific).

2.3 Reduction of nicotinamide cofactors and mimics

The following reagents were added into a 1 mL quartz cuvette: nicotinamide cofactor or mimic (**NADP$^+$**, **NAD$^+$**, or **BNA$^+$**; 0.42 mM final concentration), sodium formate (500 mM final concentration), metal catalysts (25 μM, final concentration) or artificial metalloenzyme (12.5 μM of protein, final concentration) in sodium phosphate 100 mM buffer pH 7.0. The increase of absorbance was monitored at 340 nm at 50 °C for 120 seconds (free metal catalysts) or for 1020 seconds (artificial metalloenzymes). The reaction was initiated by the addition of the catalyst. Each experiment was performed in triplicate and the average result is reported. The concentration was determined by weight for the free catalysts, and by Bradford for the artificial metalloenzymes. The TOF_{Rh} (h^{-1}) for the artificial metalloenzymes were calculated from the metal content of the protein

samples, determined by ICP-MS. The following extinction coefficients were used: 6220 M^{-1} cm^{-1} for **NAD(P)H** at 340 nm and 4800 M^{-1} cm^{-1} for **BNAH** at 340 nm.[19] 1-Benzylnicotinamide **BNA**$^+$ was prepared according to published procedures.[20]

For the Michaelis-Menten kinetics, experiments were performed as above. In each case, the average TOF_{Rh} (h^{-1}) from two measurements is shown. **NADP**$^+$ or **NAD**$^+$ were added to final concentrations of 0.025, 0.05, 0.15, 0.42, 1.2 and 2 mM. Values of K_M (μM) and TOF_{max} (h^{-1}) were calculated by non-linear regression in Prism 9 (GraphPad) using the *Michaelis-Menten enzyme kinetics* tool with parameters set to default (https://www.graphpad.com/guides/prism/latest/curve-fitting/reg_michaelis_menten_enzyme.htm).

3 Results and Discussion

3.1 Design of TbADH cysteine mutants for covalent modification

The position of the cysteine within TbADH is likely to play an important role in both the efficiency of the bioconjugation process and the activity of the embedded catalyst. To limit the experimental effort, we used a rational *in silico* approach to select suitable positions for introducing cysteine mutations, by inspecting the interactions between the protein and the covalently docked *N*-sulfonyl-ethylenediamine ligand **L1** (Figure 1a). This ligand was initially selected because it has previously been identified as one of the most efficient for the formate-driven transfer hydrogenation of nicotinamide cofactors and of imines in water, in particular when part of Ir piano-stool complexes.[21] Covalent docking of **L1** within the TbADH 5M mutant, using the C37 single cysteine as anchoring point and in the absence of the bound cofactor, suggested that the metal coordination site was oriented towards the interior of the **NADP**$^+$ binding pocket (Figure 1b), and that as a consequence **NADP**$^+$ was bound at a position different from its native site. Furthermore, non-covalent docking of the NAD(P)$^+$ mimic 1-benzylnicotinamide **BNA**$^+$ within wild-type

TbADH showed that the highest scoring docking poses depicted a flipped nicotinamide ring compared to natural cofactor binding as demonstrated by the crystal structure conformation. This results in the C4 position of the nicotinamide (involved in hydride transfer) pointing away from the catalytic zinc site (Figure 1c). This indicates that alternative positions for covalent ligand binding might be better suitable.

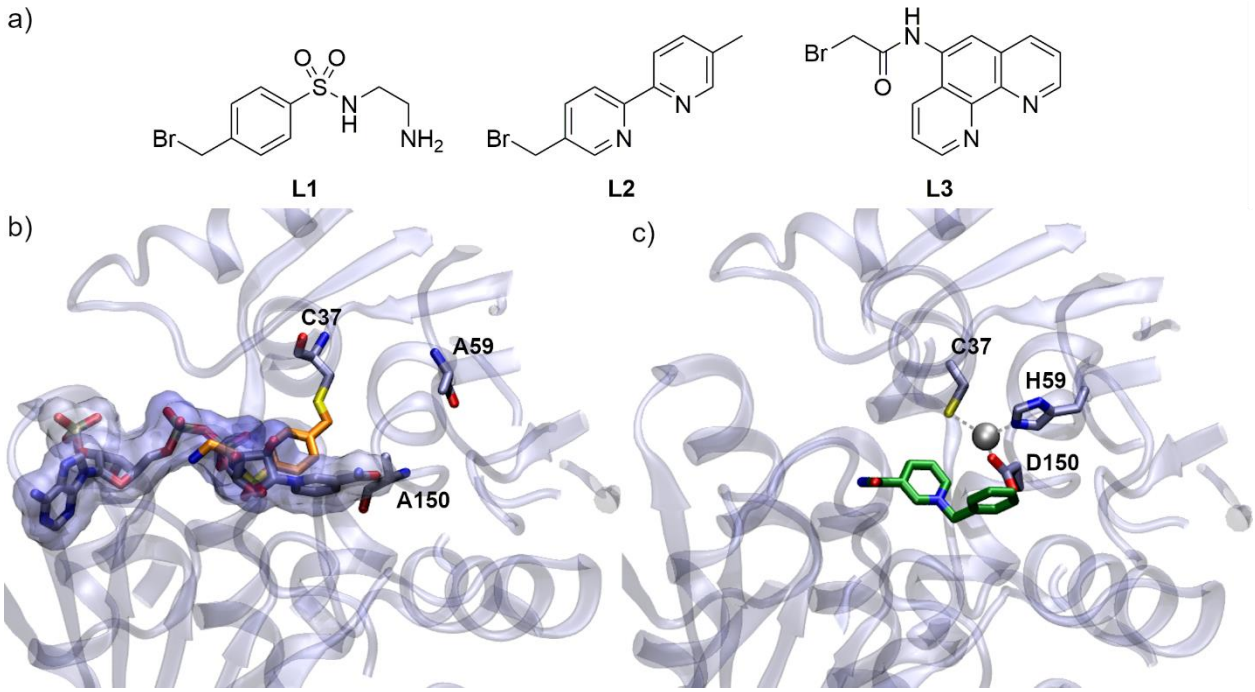

Figure 1. a) The three brominated ligands used in this study; b) Covalent docking of ligand **L1** to cysteine C37, superimposed with the $NADP^+$ cofactor crystallised within wild-type TbADH (PDB 1YKF); c) Supramolecular docking of 1-benzylnicotinamide within wild-type TbADH.

Four positions were initially chosen as potential anchoring points, based on the inspection of the TbADH crystal structure containing the $NADP^+$ cofactor.[16] The selected amino acids, 175, 178, 203 and 266 (Figure S1) were dispersed throughout the cofactor binding site. The four corresponding single cysteine mutants were created *in silico*, starting from variant TbADH 6M, devoid of the Zn binding site and of all other cysteines (6M corresponds to mutations C37A, H59A, D150A, C203S, C283A and C295A). Covalent docking of ligand **L1** at the four different positions

led to locations of the *N*-sulfonyl-ethylenediamine too far away from the hydrophobic substrate binding pocket (Figure S2). In a subsequent step, starting from the four covalently docked structures, close-lying sidechains were identified with the following properties: within a radius of 4 Å from the ligand, positioned on a loop and oriented towards the substrate binding site. Four new side-chains were identified after inspection of all the covalently docked structures and were selected for further investigation: 174, 198, 242 and 243. Cysteines were introduced at these four positions using *in silico* mutation, and ligand **L1** was covalently docked using the corresponding thiols as anchoring points. In all cases, the *N*-sulfonyl-ethylenediamine moiety was oriented towards the hydrophobic substrate binding site (Figure 2).

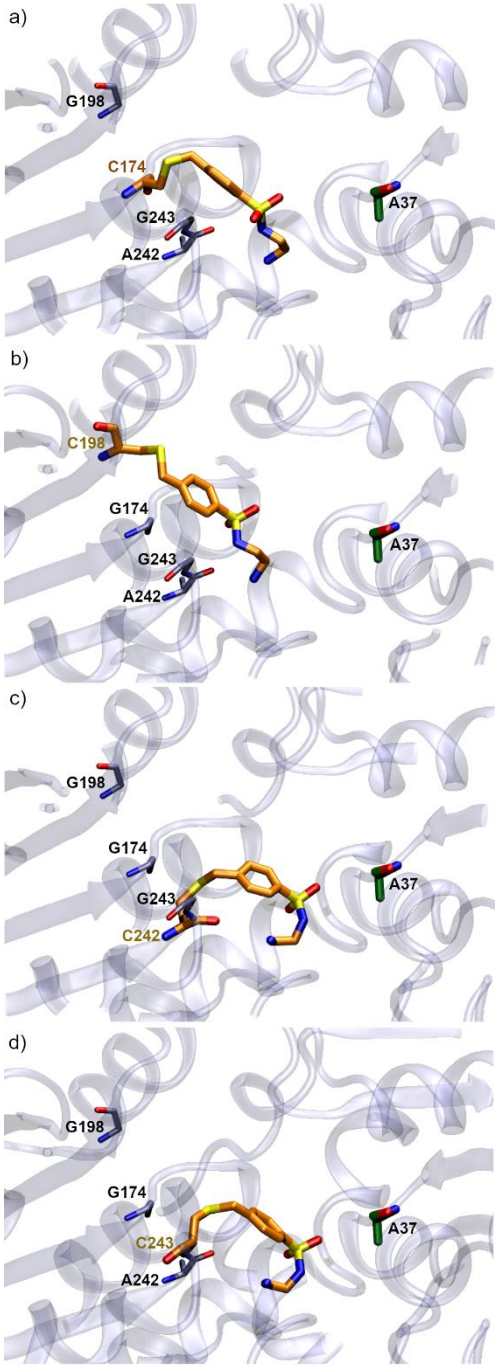

Figure 2. Covalent docking of ligand L1 to selected cysteine TbADH mutants at positions: a) C174; b) C198; c) C242; d) C243. The cysteine mutants were prepared starting from the TbADH variant 6M. The alanine at position 37, situated in the catalytic site is highlighted in green.

3.2 Bioconjugation of piano-stool metal complexes to TbADH

Single cysteine mutants were prepared experimentally at the 4 selected positions, starting from the TbADH 6M variant and introducing a seventh additional mutation, to yield: 7M-C174, 7M-C198, 7M-C242 and 7M-C243. The mutants were overexpressed in *E. coli* and purified by Strep-tag affinity chromatography. The accessibility of the cysteines for covalent labeling varied with their location and led to 48-63% labeling of the thiols with Ellman's reagent (Table S2; 69% with the previously reported TbADH 5M mutant). This low thiol availability suggested that the newly designed cysteine mutants were less accessible for covalent labeling compared to our initial design, mutant 5M with a labelled C37 cysteine in the active site.

The bioconjugation of **L1** to TbADH was carried out under optimized conditions, using 1 mg mL^{-1} protein mixed with 100 μM (4 equivalents) of the ligand over 4 h at 37 °C in Tris HCl buffer at pH 8.0. Under these conditions, it was found that cysteines at positions 198 and 242 were not efficiently labelled with the brominated ligand. On the other hand, mutants 7M-C174 and 7M-C243 readily reacted with **L1**, and in the case of the latter yielded 100 % labeling, as verified by ESI-MS (Figure S4). Interestingly, these results were more encouraging than the Ellman assay outcomes, which showed a relatively low thiol availability for the two mutants. It is possible that inaccurate protein concentrations obtained from Bradford assays led to underestimated thiol availability for the labeling of these mutants with **L1**. Following the successful labeling with the free ligand confirmed by ESI-MS, the bioconjugation of its corresponding Ir piano-stool complex to the newly designed mutants was attempted, using complex $[Cp^*Ir(\mathbf{L1})Cl]^+$. Unfortunately, under all conditions tested (variation of temperature, concentration of the reagents, contact time, etc), the contact of the protein with this metal complex led to protein precipitation and no ArMs containing complexes of **L1** could be obtained.

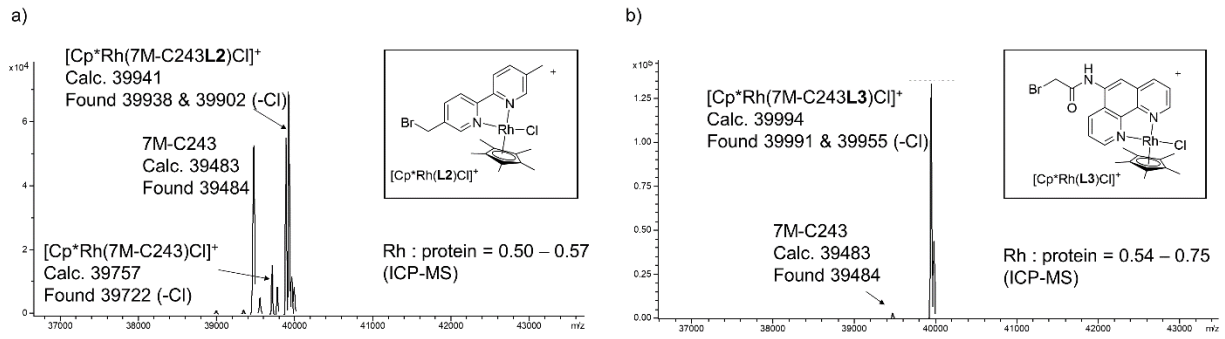

Figure 3. Mass spectrometry analysis of artificial metalloenzymes based on covalent labeling of TbADH 7M-C243 with rhodium complexes.

In addition to iridium *N*-sulfonyl-ethylenediamine, rhodium piano-stool complexes of phenanthroline and of bipyridine ligands **L2** and **L3** were also reported to be involved in redox reactions of nicotinamide cofactors and their mimics. We therefore switched to complexes [Cp*Rh(**L2**)Cl]$^+$ and [Cp*Rh(**L3**)Cl]$^+$, which we have previously shown to form active ArMs when covalently linked to cysteine C37. We reasoned that these compounds would adopt a similar orientation to ligand **L1** inside TbADH, and therefore the conclusions of the docking analysis would also apply in the case of these ligands. Labeling of 5M-C37 with **L1** and **L2** afforded similar levels of incomplete labeling; whilst labeling with **L3** was quantitative by ESI-MS. We attributed this result to the difference in reactivity between the benzyl bromide and the α-bromocarbonyl functionalities of the ligands. When the four mutants were labelled with ligand **L3**, the bioconjugation occurred more readily but similar trends were observed as for the **L1** ligand and confirmed positions 174 and 243 as the most suitable for bioconjugation (Figure S5). On the other hand, covalent labeling of 7M-C174 with the metal complexes [Cp*Rh(**L2**)Cl]$^+$ or [Cp*Rh(**L3**)Cl]$^+$ occurred in poor yield, with only a small peak corresponding to the desired bioconjugate being identified by ESI-MS. Furthermore, unspecific binding of the Cp*Rh moiety to TbADH was also observed in both cases, indicating its dissociation from the bidentate ligand

(Figure S6). Labeling of 7M-C243 with [Cp*Rh(**L2**)Cl]$^+$ occurred in better yield, but was incomplete, probably due to the low reactivity of the benzylic bromide. In contrast, the bioconjugation of **L3** to 7M-C243 *via* the bromoacetyl moiety was very efficient, with the majority of the protein forming the desired complex [Cp*Rh(7M-C243**L3**)Cl]$^+$ as a single species, as identified by ESI-MS (Figure 3). We proceeded with further testing of both these ArMs in catalysis.

3.3 Reduction of nicotinamide cofactors and mimic with ArMs

The reduction of the natural cofactors **NADP**$^+$ and **NAD**$^+$ was tested in phosphate buffer at pH 7.0 and at 50 °C, using [Cp*Rh(**L2**)Cl]$^+$ and [Cp*Rh(**L3**)Cl]$^+$ covalently bound to C243, as well as the corresponding free rhodium complexes (Table 1). As previously reported, decreased activity was obtained with all of the ArMs compared to the free complexes, due to the burial of the metal within the enzyme (entries 1 *vs* 3-4). Both native cofactors **NADP**$^+$ and **NAD**$^+$ were reduced with similar rates, irrespective of the ligand (**L2** vs **L3**) and of the anchoring position (37 vs 243). Therefore, further characterisation was focused on the use of [Cp*Rh(7M-C243**L3**)Cl]$^+$, which gave the best bioconjugation results. Similar to previously published results at position C37, bioconjugation at position C243 seemed to shield the catalyst from interaction with wild-type TbADH. In fact, upon incubation with Cp*Rh(7M-C243**L3**Cl]$^+$ for 24 hours at 50 °C, the activity of wild-type TbADH remained ~ 70% of the initial activity; whilst only 20% activity was maintained in the presence of free catalyst.[7]

This artificial metalloenzyme displayed Michaelis-Menten kinetics with both **NADP**$^+$ and **NAD**$^+$, showing an apparent K_M constant of [Cp*Rh(7M-C243**L3**)Cl]$^+$ for **NADP**$^+$ of 52 μM, which was 7.5-fold higher than K_M^{NADP+} of the native TbADH variant (Figure 4a-b).[22] In our hands, both the free complexes and the ArM were more active towards the reduction of the natural

cofactors than towards the reduction of the mimic 1-benzylnicotinamide (**BNA**$^+$; Table 1 entries 1 *vs* 7; 4-6 *vs* 8). Interestingly, the kinetics with **BNA**$^+$ did not display the hyperbolic Michaelis-Menten behaviour, suggesting a different interaction of the ArM with this substrate, which does not include the specific enzyme-substrate binding event (Figure 4c).

Table 1. Turnover frequencies (TOF_{Rh}, h^{-1}) measured for the reduction of nicotinamide compounds by artificial metalloenzymes.

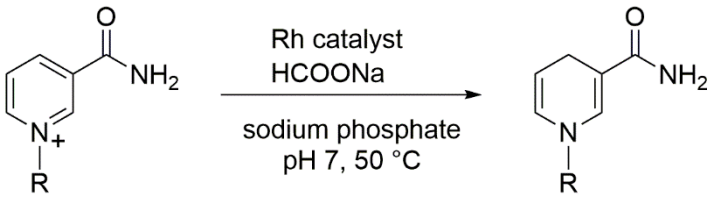

R = ribose-ADP, **NAD**$^+$
R = ribose-ADP 2'-phosphate, **NADP**$^+$
R = benzyl, **BNA**$^+$

Entry	Catalyst	Nicotinamide derivative	TOF_{Rh} (h^{-1})
1	[Cp*Rh(**L3**)Cl]$^+$	NADP$^+$	255.5 ± 7.2
2	[Cp*Rh(7M-C243**L2**)Cl]$^+$	NADP$^+$	65.5 ± 2.0
3	[Cp*Rh(5M-C37**L3**)Cl]$^+$	NADP$^+$	72.1 ± 1.6[a]
4	[Cp*Rh(7M-C243**L3**)Cl]$^+$	NADP$^+$	70.2 ± 1.9
5	Cp*Rh(**L3**)Cl]$^+$	NAD$^+$	250.3 ± 4.5
6	[Cp*Rh(7M-C243**L2**)Cl]$^+$	NAD$^+$	39.1 ± 0.9
7	[Cp*Rh(7M-C243**L3**)Cl]$^+$	NAD$^+$	71.1 ± 0.2
8	[Cp*Rh(**L3**)Cl]$^+$	BNA$^+$	59.0 ± 1.9
9	[Cp*Rh(7M-C243**L3**)Cl]$^+$	BNA$^+$	27.0 ± 4.3

Reaction conditions: Rh catalyst (12.5 μM for ArMs, 25 μM for free complexes), nicotinamide compound 0.42 mM, sodium formate 500 mM, 100 mM sodium phosphate buffer pH 7.0, 50 °C. The reaction was monitored at 340 nm for 900 s (for ArM) or 120 s (for free catalysts). The result shown is the mean ± standard error (n = 3). The extinction coefficients were 6220 M^{-1} cm^{-1} for **NAD(P)H** at 340 nm and 4800 M^{-1} cm^{-1} for **BNA**$^+$ at 340 nm. [a] Previously reported data = 74 h^{-1}.

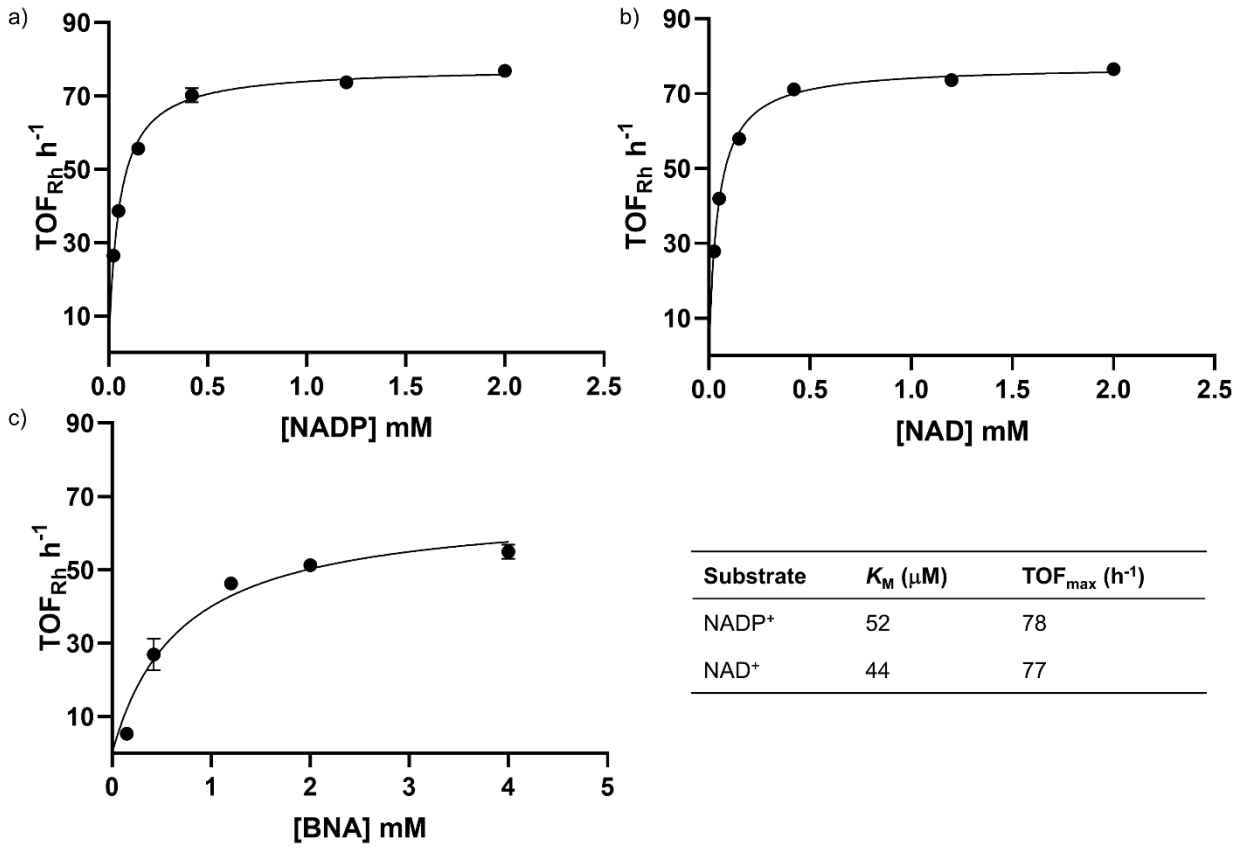

Substrate	K_M (μM)	TOF_{max} (h^{-1})
$NADP^+$	52	78
NAD^+	44	77

Figure 4. Variation of the activity of [Cp*Rh(7M-C243L3)Cl]$^+$ (displayed as TOF_{Rh}) with increasing concentration of the nicotinamide substrates: a) $NADP^+$, b) NAD^+ and c) BNA^+.

To gain insight into the binding of the nicotinamide substrates to the protein, we performed covalent docking of [Cp*Rh(**L3**)Cl]$^+$ at position C243, followed by supramolecular docking of the three substrates (**$NADP^+$**, **NAD^+**, and the **BNA^+** mimic; Figure 5). The results showed that the metal active site was mainly oriented towards the surface of the protein, blocking the access to the cofactor binding site and thus leaving little space for the nicotinamide substrates. Docking of the native cofactors to the ArM occurred towards the surface, in positions that were generally in proximity of the metal. On the other hand, docking of **BNA^+** to the ArM was less specific, showing

a higher flexibility in the binding modes of this substrate, which occurred both in the hydrophobic substrate pocket of TbADH and at the surface of the protein.

Taken together, the kinetic and the docking data suggest that the binding of the natural cofactors **NAD**$^+$ and **NADP**$^+$ to the [Cp*Rh(7M-C243**L3**)Cl]$^+$ ArM occurs at a specific binding site situated on the outer surface of the protein. This result was somewhat expected, because the cofactor binding pocket is occupied by the Cp*Rh-phenanthroline complex. Whilst the **BNA**$^+$ substrate is smaller and can be accommodated into the protein cavity, it is unlikely to bind with high affinity, whether outside or inside the protein. Given the orientation of the metal complex when covalently docked at position C243, the reduction of this substrate is also likely to take place on the surface of the protein.

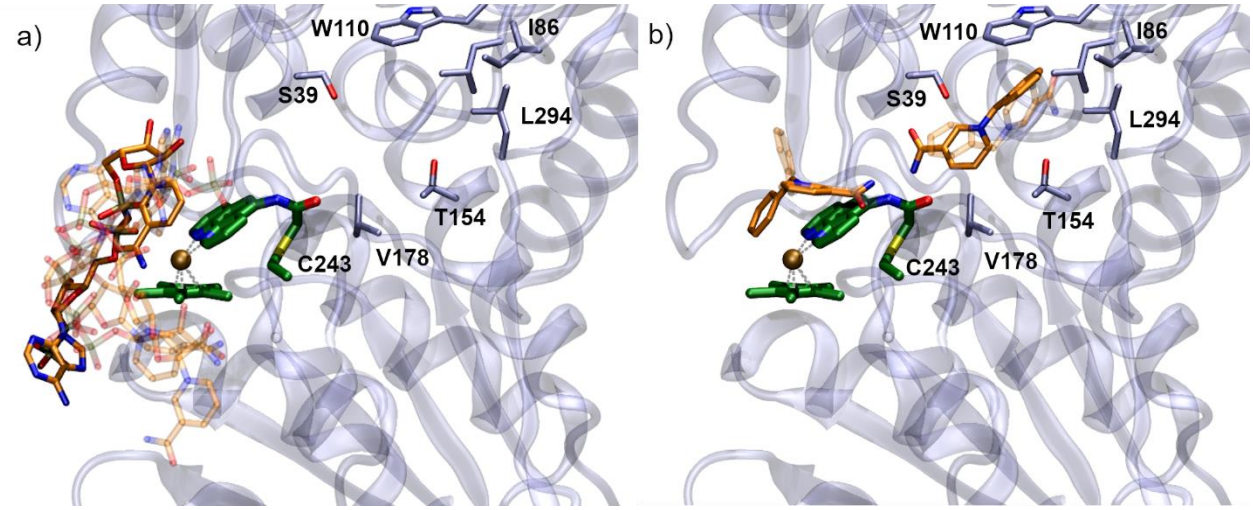

Figure 5. Covalently docked [Cp*Rh(L3)Cl]$^+$ (green licorice) at position C243 within TbADH with a) supramolecular docking of NADP$^+$ (orange licorice representation) displaying binding at the surface of the enzyme in all highest ranked docking poses and b) BNA$^+$ (orange licorice representation) displaying flexible binding modes inside the pocket and at the surface, facing the metal catalyst. The residues lining the hydrophobic substrate

binding pocket are displayed in grey. A summary of the docking results (poses, locations and distance between metal and substrate) is presented in Table S1 of the ESI.

4 Conclusions

In conclusion, we used a systematic approach to identify suitable sites for covalent bioconjugation of active piano-stool complexes to TbADH. This allowed us to design and characterise an artificial metalloenzyme that could reduce the hydrophobic 1-benzylnicotinamide mimic **BNA**$^+$, as well as the native cofactors **NADP**$^+$ and **NAD**$^+$. Docking studies suggested that the catalysis with the native cofactors occurred at the surface of the protein, where substrates were shown to bind at a different position from their native binding site. Kinetic data confirmed a binding event of the natural cofactors to the artificial metalloenzyme. On the other hand, the kinetic and docking data suggested that a typical enzyme behaviour was not observed with **BNA**$^+$, with which binding events were plausible both inside and outside the protein. Whilst there seems to be more space available for accommodating the small nicotinamide substrate in the protein cavity, compared to the much larger NAD(P)$^+$, the affinity of the TbADH catalytic site for this hydrophobic molecule is likely to be low. These results provide valuable information on further design of these ArMs, towards improving their ability to reduce hydrophobic substrates.

Supporting information. Electronic Supporting Information detailing protein bioconjugation analyses is available free of charge.

Author Information

Corresponding author

E-mail: anca.pordea@nottingham.ac.uk

Telephone: +44 (0) 115 951 4087

ORCID Anca Pordea: 0000-0001-8453-0743;

Acknowledgements

MB was funded by a studentship from the SynBio Doctoral Training Program (BBSRC). HP is funded by a studentship from the BBSRC Doctoral Training Program. We gratefully acknowledge Mr. Ben Pointer-Gleadhill for the help with ESI-TOF mass spectrometry analysis of the proteins. We also acknowledge support received from the University of Nottingham Research Green Chemicals Beacon of Excellence.

CRediT author statement

Mattias Basle: Conceptualization, Methodology, Investigation. **Henry A. W. Padley**: Conceptualization, Methodology, Investigation. **Floriane L. Martins**: Software, Methodology, Formal analysis. **Gerlof Sebastiaan Winkler**: Conceptualization, Supervision. **Christof M. Jäger**: Software, Visualisation, Supervision. **Anca Pordea**: Conceptualization, Supervision, Writing.

References

[1] F. Schwizer, Y. Okamoto, T. Heinisch, Y. Gu, M. M. Pellizzoni, V. Lebrun, R. Reuter, V. Köhler, J. C. Lewis, T. R. Ward, *Chem. Rev.* **2018**, *118*, 142-231.
[2] A. D. Liang, J. Serrano-Plana, R. L. Peterson, T. R. Ward, *Acc. Chem. Rev.* **2019**, *52*, 585-595.
[3] G. Roelfes, *Acc. Chem. Rev.* **2019**, *52*, 545-556.
[4] a) K. Oohora, A. Onoda, T. Hayashi, *Acc. Chem. Rev.* **2019**, *52*, 945-954; b) S. N. Natoli, J. F. Hartwig, *Acc. Chem. Rev.* **2019**, *52*, 326-335.
[5] a) Q. Jing, R. J. Kazlauskas, *ChemCatChem* **2010**, *2*, 953-957; b) H. M. Key, D. S. Clark, J. F. Hartwig, *J. Am. Chem. Soc.* **2015**, *137*, 8261-8268.
[6] C. K. Prier, F. H. Arnold, *J. Am. Chem. Soc.* **2015**, *137*, 13992-14006.
[7] S. Morra, A. Pordea, *Chem. Sci.* **2018**, *9*, 7447-7454.
[8] M. Peretz, L. M. Weiner, Y. Burstein, *Protein Sci.* **1997**, *6*, 1074-1083.
[9] a) T. D. Meo, W. Ghattas, C. Herrero, C. Velours, P. Minard, J. P. Mahy, R. Ricoux, A. Urvoas, *Chem. Eur. J.* **2017**, *23*, 10156-10166; b) T. Di Meo, K. Kariyawasam, W. Ghattas, M. Valerio-Lepiniec, G. Sciortino, J.-D. Maréchal, P. Minard, J.-P. Mahy, A. Urvoas, R. Ricoux, *ACS Omega* **2019**, *4*, 4437-4447.
[10] M. Bersellini, G. Roelfes, *Org. Biomol. Chem.* **2017**, *15*, 3069-3073.
[11] a) I. Zachos, C. Nowak, V. Sieber, *Curr. Opin. Chem. Biol.* **2019**, *49*, 59-66; b) C. E. Paul, I. W. C. E. Arends, F. Hollmann, *ACS Catal.* **2014**, *4*, 788-797.
[12] a) R. Ruppert, S. Herrmann, E. Steckhan, *J. Chem. Soc., Chem. Commun.* **1988**, 1150-1151; b) J. Canivet, G. Süss-Fink, P. Štěpnička, *Eur. J. Inorg. Chem.* **2007**, *2007*, 4736-4742.
[13] a) H. C. Lo, C. Leiva, O. Buriez, J. B. Kerr, M. M. Olmstead, R. H. Fish, *Inorg. Chem.* **2001**, *40*, 6705-6716; b) J. Lutz, F. Hollmann, T. V. Ho, A. Schnyder, R. H. Fish, A. Schmid, *J. Organomet.*

Chem. **2004**, *689*, 4783-4790; c) T. Knaus, C. E. Paul, C. W. Levy, S. de Vries, F. G. Mutti, F. Hollmann, N. S. Scrutton, *J. Am. Chem. Soc.* **2016**, *138*, 1033-1039; d) H. C. Lo, J. D. Ryan, J. B. Kerr, D. S. Clark, R. H. Fish, *J. Organomet. Chem.* **2017**, *839*, 38-52.

[14] a) V. Köhler, Y. M. Wilson, M. Dürrenberger, D. Ghislieri, E. Churakova, T. Quinto, L. Knörr, D. Häussinger, F. Hollmann, N. J. Turner, T. R. Ward, *Nat. Chem.* **2012**, *5*, 93; b) Y. Okamoto, V. Köhler, T. R. Ward, *J. Am. Chem. Soc.* **2016**, *138*, 5781-5784; c) Y. Okamoto, V. Köhler, C. E. Paul, F. Hollmann, T. R. Ward, *ACS Catal.* **2016**, *6*, 3553-3557.

[15] Schrödinger, LLC, New York, NY, **2016**.

[16] Y. Korkhin, A. J. Kalb, M. Peretz, O. Bogin, Y. Burstein, F. Frolow, *J. Mol. Biol.* **1998**, *278*, 967-981.

[17] M. H. M. Olsson, C. R. Søndergaard, M. Rostkowski, J. H. Jensen, *J. Chem. Theory Comput.* **2011**, *7*, 525-537.

[18] E. Harder, W. Damm, J. Maple, C. Wu, M. Reboul, J. Y. Xiang, L. Wang, D. Lupyan, M. K. Dahlgren, J. L. Knight, J. W. Kaus, D. S. Cerutti, G. Krilov, W. L. Jorgensen, R. Abel, R. A. Friesner, *J. Chem. Theory Comput.* **2016**, *12*, 281-296.

[19] Y. Tamaki, T. Morimoto, K. Koike, O. Ishitani, *Proc. Natl. Acad. Sci.* **2012**.

[20] B. Peng, C. Liu, Z. Li, J. J. Day, Y. Lu, D. J. Lefer, M. Xian, *Bioorg. Med. Chem. Lett.* **2017**, *27*, 542-545.

[21] a) S. G. Keller, M. R. Ringenberg, D. Häussinger, T. R. Ward, *Eur. J. Inorg. Chem.* **2014**, *2014*, 5860-5864; b) M. Hestericová, T. Heinisch, L. Alonso-Cotchico, J.-D. Maréchal, P. Vidossich, T. R. Ward, *Angew. Chem. Int. Ed.* **2018**, *57*, 1863-1868.

[22] Z. Findrik, Đ. Vasic'-Rački, S. Lütz, T. Daußmann, C. Wandrey, *Biotechnol. Lett.* **2005**, *27*, 1087-1095.